ANZIAM J. **62** (2020), 256–273
doi:10.1017/S1446181120000218

LINEARLY IMPLICIT ENERGY-PRESERVING FOURIER PSEUDOSPECTRAL SCHEMES FOR THE COMPLEX MODIFIED KORTEWEG–DE VRIES EQUATION

J. L. YAN[1], L. H. ZHENG[2], L. ZHU[3] and F. Q. LU[4]

(Received 6 May, 2020; accepted 9 September, 2020; first published online 12 January, 2021)

Abstract

We propose two linearly implicit energy-preserving schemes for the complex modified Korteweg–de Vries equation, based on the invariant energy quadratization method. First, a new variable is introduced and a new Hamiltonian system is constructed for this equation. Then the Fourier pseudospectral method is used for the space discretization and the Crank–Nicolson leap-frog schemes for the time discretization. The proposed schemes are linearly implicit, which is only needed to solve a linear system at each time step. The fully discrete schemes can be shown to conserve both mass and energy in the discrete setting. Some numerical examples are also presented to validate the effectiveness of the proposed schemes.

2020 *Mathematics subject classification*: primary 65M22; secondary 65M20, 65M70, 65L05.

Keywords and phrases: mass, energy, invariant energy quadratization method, Fourier pseudospectral method, complex modified Korteweg–de Vries equation.

1. Introduction

We consider the complex modified Korteweg–de Vries (CMKDV) equation with the following initial and periodic boundary conditions:

$$\begin{cases} u_t + u_{xxx} + \alpha(|u|^2 u)_x = 0, \\ u(x,0) = u_0(x), \qquad x \in [a,b], \\ \dfrac{\partial^i u}{\partial x^i}\Big|_{x=a} = \dfrac{\partial^i u}{\partial x^i}\Big|_{x=b}, \quad i = 0,1,2, \end{cases} \tag{1.1}$$

where $u(x,t)$ is a complex-valued function and α is a real constant.

[1]Department of Mathematics and Computer, Wuyi University, Wu Yi Shan 354300, China; e-mail: yanjinliang3333@163.com.
[2]Department of Information and Computer Technology, No. 1 Middle School of Nanping, Nanping 353000, China; e-mail: 413845939@qq.com.
[3]Department of Mathematics and Physics, Jiangsu University of Science and Technology, Zhenjiang 212003, China; e-mail: 38196700@qq.com.
[4]Changzhou Institute of Technology, Changzhou 213032, China; e-mail: 724075305@qq.com.

The CMKDV equation is an important mathematical model, which is used to describe the nonlinear evolution of plasma waves [15] and the propagation of transverse waves in a molecular chain model [11] and in a generalized elastic solid [5]. The CMKDV equation has the following analytical solution:

$$u(x,t) = \sqrt{\frac{2c}{\alpha}}\,\mathrm{sech}[\sqrt{c}(x - ct - x_0)]\exp(i\theta),$$

where c, x_0 and θ are given constants.

Under the periodic boundary conditions, the CMKDV equation satisfies the conservation laws (see, for example, [15])

$$\mathcal{M} = \int_a^b u\,dx, \quad \mathcal{K} = \int_a^b |u|^2\,dx, \quad \mathcal{H} = \int_a^b \left(\frac{\alpha}{2}|u|^4 - \left|\frac{\partial u}{\partial x}\right|^2\right)dx,$$

which are often named as mass, momentum and energy, respectively.

The CMKDV equation has been widely studied in the last decade both numerically and analytically. Muslu and Erabay [18] used three different split-step Fourier schemes to solve the CMKDV equation. Ismail [13] proposed a Petrov–Galerkin (P-G) method and a collocation method [14] using quintic B-spline, and analysed the linear stability of the methods. Uddina et al. [19] proposed a mesh-free method based on radial basis functions. Korkmaz and Dağ [16] used a differential quadrature method based on cosine expansion to solve the CMKDV equation. All the above methods, however, cannot precisely preserve the conservation properties of the CMKDV equation, which needs iteration at each time step.

As far as we know, there are quite a few numerical studies that focus on the energy-preserving methods. Cai and Miao [1] proposed an explicit multisymplectic Fourier pseudospectral scheme for the CMKDV equation. In a recent study, Yan and Zheng [20] derived an energy-preserving scheme and a momentum-preserving scheme by combining a finite volume element method (FVEM) and a discrete variational derivative method. But, their energy-preserving method is a nonlinear scheme, which needs to solve a nonlinear system at each time step. In this paper, we propose two linearly implicit energy-preserving schemes, which only need to solve a linear system at each time step using the invariant energy quadratization (IEQ) method [10, 21].

The IEQ method is an efficient way to construct linearly implicit energy-preserving schemes for the Hamiltonian partial differential equations (PDEs) [2, 10, 21]. About the idea of IEQ schemes, we refer to the review paper [23] and the references therein. Recently, the IEQ method has been extended in various ways; for instance, Gong [7–9] developed a class of arbitrarily high-order energy, stable Runge–Kutta (RK) methods for the gradient flow models. For more details, extensions and improvements of the IEQ method, refer to the literature (see [9, 22] and the references therein). In this paper, by introducing an auxiliary variable $q = |u|^2$, we transform the energy functional into a quadratic form and obtain an equivalent system with respect to u and q. Then we use a pseudospectral method for the space discretization and Crank–Nicolson [10]

https://doi.org/10.1017/S1446181120000218 Published online by Cambridge University Press

leap-frog [12] schemes for the time discretization. As far as we know, our schemes are efficient and can precisely conserve the discrete mass and energy.

The paper is organized as follows. In Section 2, we describe the spatial discretization of the CMKDV equation, including the IEQ method, spatial discretization and the conservation properties analysis of the semi-discrete scheme. In Section 3, we derive the fully discrete schemes using the Crank–Nicolson method and the leap-frog method in time, and analyse their conservation properties. In Section 4, some numerical examples are presented to verify the conservative properties and accuracy of our schemes, followed by some concluding remarks in Section 5.

2. Energy-preserving spatial discretization

In this section, we describe our numerical methods, including the IEQ method, spatial discretization and the conservation properties analysis of the semi-discrete scheme.

The CMKDV equation (1.1) can be written as the following Hamiltonian system:

$$u_t = -\frac{\partial}{\partial x}\left(\frac{\delta \mathcal{H}}{\delta \overline{u}}\right), \quad \mathcal{H} = \int_a^b \left(\frac{\alpha}{2}|u|^4 - |u_x|^2\right) dx, \tag{2.1}$$

where $(\bar{\cdot})$ denotes the conjugate of $(\cdot)$ and $\delta H/\delta \overline{u}$ is the variational derivative of $\mathcal{H}$, defined by

$$\frac{\delta \mathcal{H}}{\delta \overline{u}} = \frac{\partial \mathcal{H}}{\partial \overline{u}} - \frac{\partial}{\partial x}\left(\frac{\partial \mathcal{H}}{\partial \overline{u}_x}\right).$$

One intrinsic property of (2.1) is the energy conservation law

$$\frac{d\mathcal{H}}{dt} = \left(\frac{\delta \mathcal{H}}{\delta \overline{u}}, \frac{\partial u}{\partial t}\right) = -\left(\frac{\delta \mathcal{H}}{\delta \overline{u}}, \frac{\partial}{\partial x}\left(\frac{\delta \mathcal{H}}{\delta \overline{u}}\right)\right) = 0,$$

where $(\cdot, \cdot)$ is the inner product on L_2 defined by $(f(x), g(x)) = \int_a^b f(x)g(x)\,dx$.

2.1. IEQ method for the CMKDV equation In this subsection, we recall the IEQ approach introduced by Gong et al. [10].

Let $q = |u|^2 = u\overline{u}$; then the energy functional can be written as

$$\widetilde{\mathcal{H}} = \int_a^b \left(\frac{\alpha}{2}q^2 - u_x\overline{u}_x\right) dx.$$

Then system (2.1) can be rewritten as the following equivalent system:

$$\begin{cases} u_t = -(\alpha q u + u_{xx})_x, \\ q_t = \dfrac{\partial u}{\partial t}\overline{u} + u\dfrac{\partial \overline{u}}{\partial t}, \\ u(x,0) = u_0(x), \quad q(x,0) = |u(x,0)|^2. \end{cases} \tag{2.2}$$

https://doi.org/10.1017/S1446181120000218 Published online by Cambridge University Press

REMARK 2.1. One critical component of the IEQ approach is that the initial condition for q should be consistent, that is, $q(x,0) = |u(x,0)|^2$, to make (2.2) equivalent to the original CMKDV equation.

System (2.2) satisfies the following conservation laws.

PROPOSITION 2.2. *Let u be the solution of system (2.2) and assume that $[\alpha qu + u_{xx}]|_{x=a}^{b} = 0$ holds. Then u satisfies*

$$\frac{d\mathcal{M}}{dt} = 0, \quad \mathcal{M} = \int_a^b u\,dx.$$

PROOF. Under the given conditions,

$$\frac{d\mathcal{M}}{dt} = \int_a^b u_t\,dx = -\int_a^b (\alpha qu + u_{xx})_x\,dx = -[\alpha qu + u_{xx}]|_a^b = 0. \qquad \square$$

PROPOSITION 2.3. *Let u be the solution of system (2.2) and assume that $u_t\overline{u}_x|_{x=a}^{b} = 0$, $\overline{u}_t u_x|_{x=a}^{b} = 0$ hold. Then u satisfies*

$$\frac{d\widetilde{\mathcal{H}}}{dt} = 0, \quad \widetilde{\mathcal{H}} = \int_a^b \left(\frac{\alpha}{2}q^2 - u_x\overline{u}_x\right)dx.$$

PROOF. Under the given conditions,

$$\begin{aligned}
\frac{d\widetilde{\mathcal{H}}}{dt} &= \alpha(q_t, q) - (u_{xt}, \overline{u}_x) - (u_x, \overline{u}_{xt}) \\
&= \alpha(q_t, q) + (u_t, \overline{u}_{xx}) + (u_{xx}, \overline{u}_t) - u_t\overline{u}_x|_{x=a}^{b} - \overline{u}_t u_x|_{x=a}^{b} \\
&= \alpha(\overline{u}u_t + u\overline{u}_t, q) + (u_t, \overline{u}_{xx}) + (u_{xx}, \overline{u}_t) \\
&= (\alpha q\overline{u} + \overline{u}_{xx}, u_t) + (\alpha qu + u_{xx}, \overline{u}_t) \\
&= -(\alpha q\overline{u} + \overline{u}_{xx}, (\alpha qu + u_{xx})_x) - (\alpha qu + u_{xx}, (\alpha q\overline{u} + \overline{u}_{xx})_x) = 0,
\end{aligned}$$

where the skew-symmetry of $\partial/\partial x$ is used. $\square$

2.2. Spatial discretization We apply the pseudospectral method to discretize system (2.2). Let $a = x_0 < x_1 < \cdots < x_{J-1}$ denote a uniform partition of $\Omega = [a, b]$ with $h = (b-a)/J$. Then the spatial grid points are defined as $\Omega_h = \{x_j \mid j = 0, 1, \ldots, J-1\}$, where $x_j = a + jh$, $0 \le j \le J-1$. Let $\mathcal{V}_h = \{U \mid U = (U_j), x_j \in \Omega_h\}$ be the space of grid functions defined on Ω_h. For any two grid functions $u, v \in \mathcal{V}_h$, we define the discrete inner product as follows:

$$(u, v)_h = h\sum_{i=0}^{J-1} u_i v_i.$$

The crucial step of the pseudospectral method is to approximate the partial differential operators. The first-order derivative ∂/∂_x and the second-order derivative ∂^2/∂_x^2 are approximated by the Fourier spectral differential matrices D_1 and D_2,

https://doi.org/10.1017/S1446181120000218 Published online by Cambridge University Press

respectively [4]. Here, D_1 is a $J \times J$ skew-symmetric matrix with elements

$$(D_1)_{m,n} = \begin{cases} \dfrac{(-1)^{m+n}}{2} \cot\left(\dfrac{\omega(x_m - x_n)}{2}\right), & m \neq n, \\ 0, & m = n \end{cases}$$

and D_2 is a $J \times J$ symmetric matrix with elements

$$(D_2)_{m,n} = \begin{cases} \dfrac{1}{2}\omega^2(-1)^{m+n+1} \dfrac{1}{\sin^2(\omega(x_m - x_n)/2)}, & m \neq n, \\ -\omega^2 \dfrac{J^2+2}{12}, & m = n, \end{cases}$$

where $\omega = 2\pi/(b-a)$. In general, the following result holds.

THEOREM 2.4. *For the spectral differentiation matrices D_k and $(D_1)^k$,*

$$(D_k)_{m,n} = (D_1^k)_{m,n} + (-1)^{m+n} \frac{\omega^k}{2J}\left[\left(i\frac{J}{2}\right)^k + \left(-i\frac{J}{2}\right)^k\right].$$

In particular, $D_k = (D_1)^k$ if k is an odd number.

The proof can be found in the paper by Chen and Qin [4].

Then we discretize the CMKDV equation (2.2) using the Fourier pseudospectral method in space; a semi-discrete system is obtained:

$$\begin{cases} U_t = -D_1(\alpha Q U + D_2 U), \\ Q_t = U_t \overline{U} + U \overline{U}_t. \end{cases} \tag{2.3}$$

2.3. Conservative properties of the semi-discrete scheme In this subsection, we analyse the conservative properties of the semi-discrete system (2.3).

THEOREM 2.5. *Let U be the solution of system (2.3) and assume that it satisfies discrete periodic boundary conditions. Then U satisfies*

$$\frac{dM}{dt} = 0, \quad M = \frac{\alpha}{2}(U, \mathbf{1})_h, \quad U \in V_h.$$

PROOF. Under the given conditions,

$$\frac{dM}{dt} = (U_t, \mathbf{1})_h = -(D_1(\alpha Q U + D_2 U), \mathbf{1})_h = -\mathbf{1}^T D_1(\alpha Q U + D_2 U) = 0. \qquad \square$$

THEOREM 2.6. *Let U be the solution of system (2.3) and assume that $U_t D_1 \overline{U}|_{x=a}^b = 0$ and $\overline{U}_t D_1 U|_{x=a}^b = 0$ hold. Then U satisfies*

$$\frac{dH}{dt} = 0, \quad H = \frac{\alpha}{2}(Q, Q)_h + (\overline{U}, D_2 U)_h, \quad U, Q \in V_h.$$

https://doi.org/10.1017/S1446181120000218 Published online by Cambridge University Press

PROOF. Under the given conditions,

$$\begin{aligned}\frac{dH}{dt} &= \alpha(Q_t, Q)_h + (U_t, D_2\overline{U})_h + (\overline{U}_t, D_2U)_h\\ &= \alpha(U_t\overline{U} + U\overline{U}_t, Q)_h + (U_t, D_2\overline{U})_h + (\overline{U}_t, D_2U)_h\\ &= (\alpha\overline{U}Q, U_t)_h + (\alpha UQ, \overline{U}_t)_h + (D_2\overline{U}, U_t)_h + (D_2U, \overline{U}_t)_h\\ &= (\alpha\overline{U}Q + D_2\overline{U}, U_t)_h + (\alpha UQ + D_2U, \overline{U}_t)_h.\end{aligned}$$

Substituting (2.3) and its conjugate into the following equation

$$\begin{aligned}\frac{dH}{dt} &= (\alpha\overline{U}Q + D_2\overline{U}, U_t)_h + (\alpha UQ + D_2U, \overline{U}_t)_h\\ &= -(\alpha\overline{U}Q + D_2\overline{U}, D_1(\alpha QU + D_2U))_h - (\alpha UQ + D_2U, D_1(\alpha\overline{U}Q + D_2\overline{U}))_h\\ &= -(\overline{G}, D_1G)_h - (G, D_1\overline{G})_h = 0,\end{aligned}$$

where $G = \alpha QU + D_2U$. □

3. Energy-preserving temporal discretization

In this section, we turn to the temporal discretization of the semi-discrete system (2.3).

For a positive integer N, We define the time step $\tau = T/N$. The grid points in space and time are given by $\Omega_h^\tau = \Omega_h \times \Omega_\tau$, where $\Omega_\tau = \{t_n \mid t_n = n\tau, n = 0, 1, \ldots, N\}$. Given a grid function $U = \{U_j^n \mid (x_j, t_n) \in \Omega_h^\tau\}$, we denote

$$\delta_t^+ U^n = \frac{U^{n+1} - U^n}{\tau}, \quad \widetilde{U}^{n+(1/2)} = \frac{3U^n - U^{n-1}}{2}, \quad U^{n+(1/2)} = \frac{U^n + U^{n+1}}{2},$$
$$\delta_t^{\langle 1\rangle} U^n = \frac{U^{n+1} - U^{n-1}}{2\tau}, \quad A_{\hat{t}} U^n = \frac{U^{n+1} + U^{n-1}}{2}, \quad Q^{n+(1/2)} = \frac{Q^{n+1} + Q^n}{2}.$$

For simplicity, we denote $u_j^n = u(x_j, t_n)$ and U_j^n as the exact value of $u(x, t)$ and its numerical approximation at (x_j, t_n), respectively.

3.1. Linearly implicit Crank–Nicolson scheme We discretize the semi-discrete system (2.3) using a combination of the Crank–Nicolson method and the Adams–Bashforth method [10] in time, to obtain a fully discrete scheme:

$$\begin{cases}\delta_t^+ U^n = -D_1(\alpha Q^{n+(1/2)}\widetilde{U}^{n+(1/2)} + D_2U^{n+(1/2)}),\\ \delta_t^+ Q^n = \delta_t^+ U^n\widetilde{\overline{U}}^{n+(1/2)} + \widetilde{U}^{n+(1/2)}\delta_t^+\overline{U}^n.\end{cases} \tag{3.1}$$

THEOREM 3.1. *Let U^n be the solution of system (3.1) and assume that it satisfies discrete periodic boundary conditions. Then U^n satisfies*

$$\delta_t^+ M^n = 0, \quad M^n = \frac{\alpha}{2}(U^n, \mathbf{1})_h, \quad U^n \in \mathbb{V}_h.$$

https://doi.org/10.1017/S1446181120000218 Published online by Cambridge University Press

PROOF. Under the given conditions,

$$\begin{aligned}\delta_t^+ M^n &= (\delta_t^+ U^n, \mathbf{1})_h \\ &= -(D_1(\alpha Q^{n+(1/2)}\widetilde{U}^{n+(1/2)} + D_2 U^{n+(1/2)}), \mathbf{1})_h \\ &= -\mathbf{1}^T D_1(\alpha Q^{n+(1/2)}\widetilde{U}^{n+(1/2)} + D_2 U^{n+(1/2)}) = 0.\end{aligned}$$

□

THEOREM 3.2. *Let U^n be as in Theorem 3.1 and assume that $\delta_t^+ U^n D_1 \overline{U}^n|_{x=a}^b = 0$ and $\delta_t^+ \overline{U}^n D_1 U^n|_{x=a}^b = 0$ hold. Then U^n satisfies*

$$\delta_t^+ \widetilde{H}^n = 0, \quad \widetilde{H}^n = \frac{\alpha}{2}(Q^n, Q^n)_h + (\overline{U}^n, D_2 U^n)_h, \quad U^n, Q^n \in \mathbb{V}_h.$$

PROOF. Under the given conditions,

$$\begin{aligned}\delta_t^+ \widetilde{H}^n &= \frac{1}{\tau}\Big[\frac{\alpha}{2}[(Q^{n+1}, Q^{n+1})_h - (Q^n, Q^n)_h] + [(\overline{U}^{n+1}, D_2 U^{n+1})_h - (\overline{U}^n, D_2 U^n)_h]\Big] \\ &= \frac{\alpha}{2\tau}[(Q^{n+1}, Q^{n+1})_h + (Q^{n+1}, Q^n)_h - (Q^n, Q^{n+1})_h - (Q^n, Q^n)_h] \\ &\quad + \frac{1}{2\tau}[(U^{n+1}, D_2\overline{U}^{n+1})_h + (U^{n+1}, D_2\overline{U}^n)_h - (U^n, D_2\overline{U}^{n+1})_h - (U^n, D_2\overline{U}^n)_h \\ &\quad + (\overline{U}^{n+1}, D_2 U^{n+1})_h + (\overline{U}^{n+1}, D_2 U^n)_h - (\overline{U}^n, D_2 U^{n+1})_h - (\overline{U}^n, D_2 U^n)_h] \\ &= \frac{\alpha}{2\tau}(Q^{n+1} - Q^n, Q^{n+1} + Q^n)_h + \frac{1}{2\tau}[(U^{n+1} - U^n, D_2(\overline{U}^{n+1} + \overline{U}^n))_h \\ &\quad + (\overline{U}^{n+1} - \overline{U}^n, D_2(U^{n+1} + U^n))_h] \\ &= \alpha(\delta_t^+ Q^n, Q^{n+(1/2)})_h + (\delta_t^+ U^n, D_2\overline{U}^{n+(1/2)})_h + (\delta_t^+ \overline{U}^n, D_2 U^{n+(1/2)})_h \\ &= \alpha(\delta_t^+ U^n \widetilde{\overline{U}}^{n+(1/2)} + \widetilde{U}^{n+(1/2)}\delta_t^+ \overline{U}^n, Q^{n+(1/2)})_h + (\delta_t^+ U^n, D_2\overline{U}^{n+(1/2)})_h \\ &\quad + (\delta_t^+ \overline{U}^n, D_2 U^{n+(1/2)})_h \\ &= (\alpha\widetilde{\overline{U}}^{n+(1/2)} Q^{n+(1/2)} + D_2\overline{U}^{n+(1/2)}, \delta_t^+ U^n)_h \\ &\quad + (\alpha\widetilde{U}^{n+(1/2)}Q^{n+(1/2)} + D_2 U^{n+(1/2)}, \delta_t^+ \overline{U}^n)_h.\end{aligned}$$

Substituting (3.1) and its conjugate into the following equation

$$\begin{aligned}\delta_t^+ \widetilde{H}^n &= (\alpha\widetilde{\overline{U}}^{n+(1/2)} Q^{n+(1/2)} + D_2\overline{U}^{n+(1/2)}, \delta_t^+ U^n)_h \\ &\quad + (\alpha\widetilde{U}^{n+(1/2)}Q^{n+(1/2)} + D_2 U^{n+(1/2)}, \delta_t^+ \overline{U}^n)_h \\ &= -(\alpha\widetilde{\overline{U}}^{n+(1/2)} Q^{n+(1/2)} + D_2\overline{U}^{n+(1/2)}, D_1(\alpha\widetilde{U}^{n+(1/2)}Q^{n+(1/2)} + D_2 U^{n+(1/2)}))_h \\ &\quad - (\alpha\widetilde{U}^{n+(1/2)}Q^{n+(1/2)} + D_2 U^{n+(1/2)}, D_1(\alpha\widetilde{\overline{U}}^{n+(1/2)} Q^{n+(1/2)} + D_2\overline{U}^{n+(1/2)}))_h \\ &= -(\overline{G}^n, D_1 G^n)_h - (G^n, D_1\overline{G}^n)_h = 0,\end{aligned}$$

where $G^n = \alpha\widetilde{U}^{n+(1/2)}Q^{n+(1/2)} + D_2 U^{n+(1/2)}$. □

https://doi.org/10.1017/S1446181120000218 Published online by Cambridge University Press

3.2. Linearly implicit leap-frog scheme We discretize the semi-discrete system (2.3) using the leap-frog method [12] in time; thus, a fully discrete scheme is obtained:

$$\begin{cases} \delta_t^{\langle 1\rangle} U^n = -D_1(\alpha A_{\hat{\imath}} Q^n U^n + D_2 A_{\hat{\imath}} U^n), \\ \delta_t^{\langle 1\rangle} Q^n = \delta_t^{\langle 1\rangle} U^n \overline{U}^n + U^n \delta_t^{\langle 1\rangle} \overline{U}^n. \end{cases} \tag{3.2}$$

THEOREM 3.3. *Let U^n be the solution of (3.2) and assume that it satisfies the discrete periodic boundary conditions. Then U^n satisfies*

$$\delta_t^{\langle 1\rangle} M^n = 0, \quad M^n = \frac{\alpha}{2}(U^n, \mathbf{1})_h, \quad U^n \in \mathbb{V}_h.$$

PROOF. The proof is similar to that of Theorem 3.1. □

THEOREM 3.4. *Let U^n be as in Theorem 3.3 and assume that $\delta_t^{\langle 1\rangle} U^n D_1 \overline{U}^n|_{x=a}^b = 0$ and $\delta_t^{\langle 1\rangle} \overline{U}^n D_1 U^n|_a^b = 0$ hold. Then U^n satisfies*

$$\delta_t^{\langle 1\rangle} \widetilde{H}^n = 0, \quad \widetilde{H}^n = \frac{\alpha}{2}(Q^n, Q^n)_h + (\overline{U}^n, D_2 U^n)_h, \quad U^n, Q^n \in \mathbb{V}_h.$$

PROOF. Under the given conditions,

$$\begin{aligned} \delta_t^{\langle 1\rangle} \widetilde{H}^n &= \frac{1}{2\tau}\left\{\frac{\alpha}{2}[(Q^{n+1}, Q^{n+1})_h - (Q^{n-1}, Q^{n-1})_h] + [(\overline{U}^{n+1}, D_2 U^{n+1})_h - (\overline{U}^{n-1}, D_2 U^{n-1})_h]\right\} \\ &= \frac{\alpha}{4\tau}[(Q^{n+1}, Q^{n+1})_h + (Q^{n+1}, Q^{n-1})_h - (Q^{n-1}, Q^{n+1})_h - (Q^{n-1}, Q^{n-1})_h] \\ &\quad + \frac{1}{4\tau}[(U^{n+1}, D_2 \overline{U}^{n+1})_h + (U^{n+1}, D_2 \overline{U}^{n-1})_h - (U^{n-1}, D_2 \overline{U}^{n+1})_h - (U^{n-1}, D_2 \overline{U}^{n-1})_h \\ &\quad + (\overline{U}^{n+1}, D_2 U^{n+1})_h + (\overline{U}^{n+1}, D_2 U^{n-1})_h - (\overline{U}^{n-1}, D_2 U^{n+1})_h - (\overline{U}^{n-1}, D_2 U^{n-1})_h] \\ &= \frac{\alpha}{4\tau}(Q^{n+1} - Q^{n-1}, Q^{n+1} + Q^{n-1})_h + \frac{1}{4\tau}[(U^{n+1} - U^{n-1}, D_2(\overline{U}^{n+1} + \overline{U}^{n-1}))_h \\ &\quad + (\overline{U}^{n+1} - \overline{U}^{n-1}, D_2(U^{n+1} + U^{n-1}))_h] \\ &= \alpha(\delta_t^{\langle 1\rangle} Q^n, A_{\hat{\imath}} Q^n)_h + (\delta_t^{\langle 1\rangle} U^n, D_2 A_{\hat{\imath}} \overline{U}^n)_h + (\delta_t^{\langle 1\rangle} \overline{U}^n, D_2 A_{\hat{\imath}} U^n)_h \\ &= \alpha(\delta_t^{\langle 1\rangle} U^n \overline{U}^n + U^n \delta_t^{\langle 1\rangle} \overline{U}^n, A_{\hat{\imath}} Q^n)_h + (\delta_t^{\langle 1\rangle} U^n, D_2 A_{\hat{\imath}} \overline{U}^n)_h + (\delta_t^{\langle 1\rangle} \overline{U}^n, D_2 A_{\hat{\imath}} U^n)_h \\ &= (\alpha \overline{U}^n A_{\hat{\imath}} Q^n + D_2 A_{\hat{\imath}} \overline{U}^n, \delta_t^{\langle 1\rangle} U^n)_h + (\alpha U^n A_{\hat{\imath}} Q^n + D_2 A_{\hat{\imath}} U^n, \delta_t^{\langle 1\rangle} \overline{U}^n)_h. \end{aligned}$$

Substituting (3.2) and its conjugate into the following equation

$$\begin{aligned} \delta_t^{\langle 1\rangle} \widetilde{H}^n &= (\alpha \overline{U}^n A_{\hat{\imath}} Q^n + D_2 A_{\hat{\imath}} \overline{U}^n, \delta_t^{\langle 1\rangle} U^n)_h + (\alpha U^n A_{\hat{\imath}} Q^n + D_2 A_{\hat{\imath}} U^n, \delta_t^{\langle 1\rangle} \overline{U}^n)_h \\ &= -(\alpha \overline{U}^n A_{\hat{\imath}} Q^n + D_2 A_{\hat{\imath}} \overline{U}^n, D_1(\alpha U^n A_{\hat{\imath}} Q^n + D_2 A_{\hat{\imath}} U^n))_h \\ &\quad - (\alpha U^n A_{\hat{\imath}} Q^n + D_2 A_{\hat{\imath}} U^n, D_1(\alpha \overline{U}^n A_{\hat{\imath}} Q^n + D_2 A_{\hat{\imath}} \overline{U}^n))_h \\ &= -(\overline{G}^n, D_1 G^n)_h - (G^n, D_1 \overline{G}^n)_h = 0, \end{aligned}$$

where $G^m = \alpha U^m A_{\hat{\imath}} Q^m + D_2 A_{\hat{\imath}} U^m$. □

https://doi.org/10.1017/S1446181120000218 Published online by Cambridge University Press

Algorithm 1 LIRK4

$$
\begin{aligned}
K_1 &= u_n,\\
K_2 &= u_n + h\{(1/4)\mathcal{L}K_2 + (1/4)\mathcal{N}(K_1)\},\\
K_3 &= u_n + h\{(1/2)\mathcal{L}K_2 + (1/4)\mathcal{L}K_3 - (1/4)\mathcal{N}(K_1) + \mathcal{N}(K_2)\},\\
K_4 &= u_n + h\{(17/50)\mathcal{L}K_2 - (1/25)\mathcal{L}K_3 + (1/4)\mathcal{L}K_4\\
&\quad - (13/100)\mathcal{N}(K_1) + (43/75)\mathcal{N}(K_2) + (8/75)\mathcal{N}(K_3)\},\\
K_5 &= u_n + h\{(371/1360)\mathcal{L}K_2 - (137/2720)\mathcal{L}K_3 + (15/544)\mathcal{L}K_4\\
&\quad + (1/4)\mathcal{L}K_5 - (6/85)\mathcal{N}(K_1) + (42/85)\mathcal{N}(K_2)\\
&\quad + (179/1360)\mathcal{N}(K_3) - (15/272)\mathcal{N}(K_4)\},\\
K_6 &= u_n + h\{(25/24)\mathcal{L}K_2 - (49/48)\mathcal{L}K_3 + (125/16)\mathcal{L}K_4 - (85/12)\mathcal{L}K_5\\
&\quad + (1/4)\mathcal{L}K_6 + (79/24)\mathcal{N}(K_2) - (5/8)\mathcal{N}(K_3) + (25/2)\mathcal{N}(K_4)\\
&\quad - (85/6)\mathcal{N}(K_5)\},\\
u_{n+1} &= u_n + h\{(25/24)\mathcal{L}K_2 - (49/48)\mathcal{L}K_3 + (125/16)\mathcal{L}K_4 - (85/12)\mathcal{L}K_5\\
&\quad + (1/4)\mathcal{L}K_6 + (25/24)\mathcal{N}(K_2) - (49/48)\mathcal{N}(K_3) + (125/16)\mathcal{N}(K_4)\\
&\quad - (85/12)\mathcal{N}(K_5) + (1/4)\mathcal{N}(K_6)\}.
\end{aligned}
$$

REMARK 3.5. The proposed schemes are two three-level energy-preserving schemes. The initial value U^1 is obtained by the nonlinear scheme

$$\delta_m^+ U^m = -D_1\left[\frac{\alpha}{2}(|U^{m+1}|^2 + |U^m|^2)U^{m+(1/2)} + D_2 U^{m+(1/2)}\right], \tag{3.4}$$

which is constructed by the discrete variational derivative method [6]. One can prove that scheme (3.4) precisely conserves the discrete mass and energy (for more details, refer to [20] and the references therein).

REMARK 3.6. In the following, the Crank–Nicolson scheme is named "linear1", the leap-frog scheme is named "linear2" and the above nonlinear scheme is named "nonlinear".

In addition, we also compare the proposed methods with the fourth-order linearly implicit Runge–Kutta method (LIRK4) [3, 17] (see Algorithm 1). To this end, we split the semi-discrete system of (1.1) into the form

$$U_t = -D_3 U - \alpha D_1(|U|^2 U) = \mathcal{L}U + \mathcal{N}(U),$$

where $\mathcal{L}$ and $\mathcal{N}$ are linear and nonlinear operators, respectively.

4. Numerical experiments

In this section, we present some numerical examples to validate the accuracy, conservative properties and the efficiency of the proposed schemes.

https://doi.org/10.1017/S1446181120000218 Published online by Cambridge University Press

In the following, we will use the following error norms to measure the error of the proposed schemes:

$$L_1 = \sum_{i=0}^{J-1} |U_i^n - u_i^n|\, h, \quad L_2 = \Big(\sum_{i=0}^{J-1} |U_i^n - u_i^n|^2\, h \Big)^{1/2}, \quad L_\infty = \max_{0\le i\le J-1} |U_i^n - u_i^n|.$$

The convergence rate is calculated by $\log_2(e_h/e_{h/2})$, where e_h and $e_{h/2}$ denote the error norms of grid spacings h and $h/2$, respectively.

4.1. Single solitary wave The CMKDV equation has the solitary wave solution

$$u(x,t) = \sqrt{\frac{2c}{\alpha}}\, \mathrm{sech}[\sqrt{c}(x - ct - x_0)] \exp(i\theta), \tag{4.1}$$

where α, c, θ and x_0 are given constants. The exact solution represents a solitary wave with amplitude $\sqrt{2c/\alpha}$, initially located at $x = x_0$, and moved to the right with velocity c. The initial condition can be obtained by setting $t = 0$ in (4.1):

$$u(x,0) = \sqrt{c}\, \mathrm{sech}[\sqrt{c}(x - x_0)] \exp(i\theta).$$

Firstly, we consider the accuracy of the proposed scheme in space and time. To this end, we set $\alpha = 2$, $c = 1$, $\theta = \pi/2$ $x \in [-30, 30]$ and $T = 1$. Tables 1 and 2 show that the spatial errors are very small, and the errors are dominated by the time discretization errors. The results further confirm that, for the sufficiently smooth problem, the Fourier pseudospectral method can reach an arbitrary order of accuracy. Tables 3 and 4 clearly indicate that the proposed methods are of second-order accuracy in time. Figure 1 also compares the computation times of the proposed schemes and the nonlinear scheme. The result shows that our schemes are more efficient than the nonlinear scheme.

TABLE 1. Spatial errors and convergence orders of the linear1 with $\tau = 1 \times 10^{-8}$ and $N = 1000$.

h	L_1	Order	L_2	Order	L_∞	Order
2	4.2106×10^{-5}	—	9.5014×10^{-6}	—	3.9120×10^{-6}	—
1	1.0013×10^{-5}	2.0722	2.5871×10^{-6}	1.8768	1.1898×10^{-6}	1.7172
1/2	2.4821×10^{-7}	5.3342	7.2634×10^{-8}	5.1545	3.8466×10^{-8}	4.9510
1/4	4.8108×10^{-11}	12.3330	1.5494×10^{-11}	12.1947	9.3862×10^{-12}	12.0008

TABLE 2. Spatial errors and convergence orders of the linear2 with $\tau = 1 \times 10^{-8}$ and $N = 1000$.

h	L_1	Order	L_2	Order	L_∞	Order
2	4.2106×10^{-5}	—	9.5014×10^{-6}	—	3.9120×10^{-6}	—
1	1.0013×10^{-5}	2.0722	2.5871×10^{-6}	1.8768	1.1898×10^{-6}	1.7172
1/2	2.4821×10^{-7}	5.3342	7.2633×10^{-8}	5.1546	3.8466×10^{-8}	4.9510
1/4	4.6893×10^{-11}	12.3699	1.4880×10^{-11}	12.2530	8.2789×10^{-12}	12.1819

https://doi.org/10.1017/S1446181120000218 Published online by Cambridge University Press

TABLE 3. Temporal errors and convergence orders of the linear1 with $h = 1/5$ and $T = 1$.

τ	L_1	Order	L_2	Order	L_∞	Order
1/5	5.6900×10^{-2}	—	2.3600×10^{-2}	—	1.7500×10^{-2}	—
1/10	1.6600×10^{-2}	1.7772	6.3000×10^{-3}	1.9054	4.8000×10^{-3}	1.8662
1/20	4.6000×10^{-3}	1.8515	1.6000×10^{-3}	1.9773	1.3000×10^{-3}	1.8845
1/40	1.2000×10^{-3}	1.9386	4.2083×10^{-4}	1.9268	3.2121×10^{-4}	2.0169
1/80	3.1358×10^{-4}	1.9361	1.0643×10^{-4}	1.9833	8.1304×10^{-5}	1.9821

TABLE 4. Temporal errors and convergence orders of the linear2 with $h = 1/5$ and $T = 1$.

τ	L_1	Order	L_2	Order	L_∞	Order
1/5	4.3900×10^{-2}	—	1.6800×10^{-2}	—	1.2900×10^{-2}	—
1/10	1.1600×10^{-2}	1.9201	3.8000×10^{-3}	2.1444	2.5000×10^{-3}	2.3674
1/20	3.2000×10^{-3}	1.8580	9.6412×10^{-4}	1.9787	6.1934×10^{-4}	2.0131
1/40	8.8225×10^{-4}	1.8588	2.4289×10^{-4}	1.9886	1.5452×10^{-4}	2.0029
1/80	2.3818×10^{-4}	1.8891	6.1019×10^{-5}	1.9930	3.8682×10^{-5}	1.9981

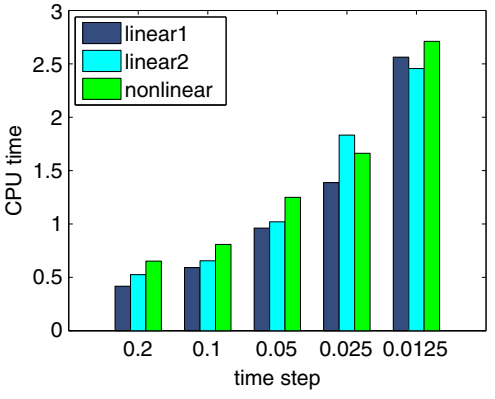

FIGURE 1. Comparison of computation times of the linear1, linear2 and nonlinear schemes.

Secondly, we compare the proposed methods with the existing methods, such as the LIRK4 method, the Petrov–Galerkin method [13], FVEM [20] and the nonlinear scheme (3.4). The computations are conducted on $[-30, 30]$ until $T = 20$. Given the parameters $h = 1/2$, $\tau = 0.01$ and $\theta = \pi/4$, we compute the L_∞ errors between the exact solution and the numerical solutions obtained by the above methods, respectively, as shown in Table 5. For $t \in [0, 20]$, the numerical results obtained by using the pseudospectral method are much better than those of the Petrov–Galerkin method [13] and the FVEM [20]. The numerical solution of the linear1 and the related exact solution over $t \in [0, 20]$ are presented in Figure 2. It is shown that the numerical

https://doi.org/10.1017/S1446181120000218 Published online by Cambridge University Press

TABLE 5. L_∞ errors of the proposed methods and the methods in references.

T	linear1	linear2	nonlinear	LIRK4	P-G [13]	FVEM [20]
0	0	0	0	0	0	0
5	1.7952×10^{-4}	4.2364×10^{-5}	4.8423×10^{-5}	1.7041×10^{-6}	1.1383×10^{-3}	9.5199×10^{-3}
10	3.6041×10^{-4}	7.1382×10^{-5}	9.6416×10^{-5}	2.6759×10^{-6}	1.9419×10^{-3}	1.6921×10^{-2}
15	5.4242×10^{-4}	1.1120×10^{-4}	1.4427×10^{-4}	3.8063×10^{-6}	2.8816×10^{-3}	2.2182×10^{-2}
20	7.3118×10^{-4}	1.5376×10^{-4}	1.9249×10^{-4}	9.0831×10^{-6}	3.8092×10^{-3}	2.7312×10^{-2}

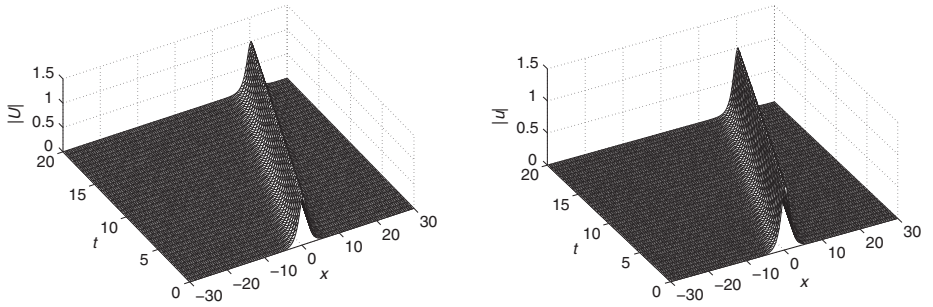

FIGURE 2. Numerical solution of the linear1 and the related exact solution when $h = 1/2$, $\tau = 0.01$ and $\theta = \pi/4$.

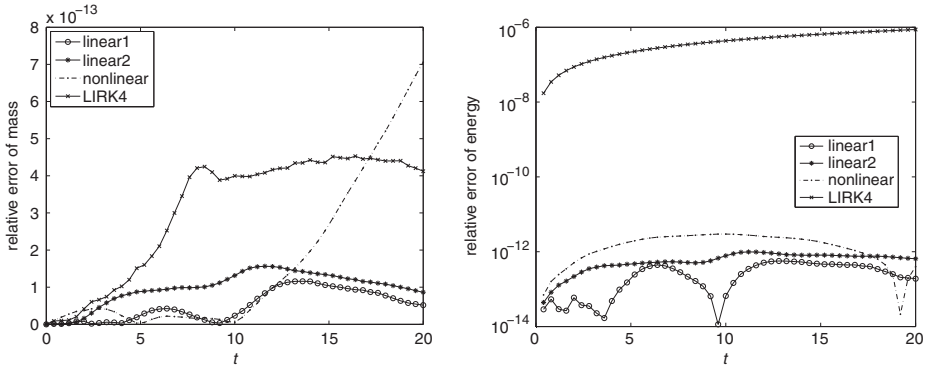

FIGURE 3. Time evolution of the relative errors of discrete mass and energy. Left: $|M(t) - M(0)|/M(0)$; right: $\log(|\widetilde{H}(t) - \widetilde{H}(0)|/\widetilde{H}(0))$.

approximation is in good agreement with the exact solution. The relative errors of the discrete mass and energy are also plotted in Figure 3. Notice that the the LIRK4 method can conserve discrete energy within 10^{-6}. In contrast, the proposed energy-preserving schemes conserve the discrete mass and energy to 10^{-13}, which is strict conservation in a numerical sense and conform to the theoretical results.

https://doi.org/10.1017/S1446181120000218 Published online by Cambridge University Press

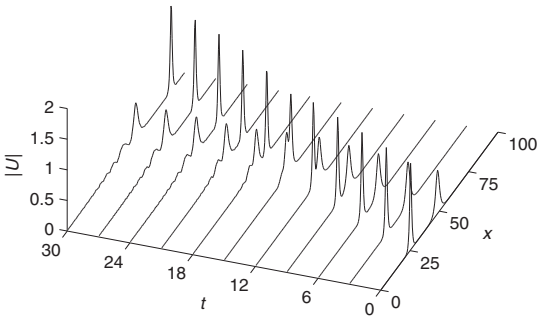

FIGURE 4. Numerical solution of the linear1 when $h = 1/2$, $\tau = 0.01$, $\theta_1 = 0$ and $\theta_1 = \pi/2$.

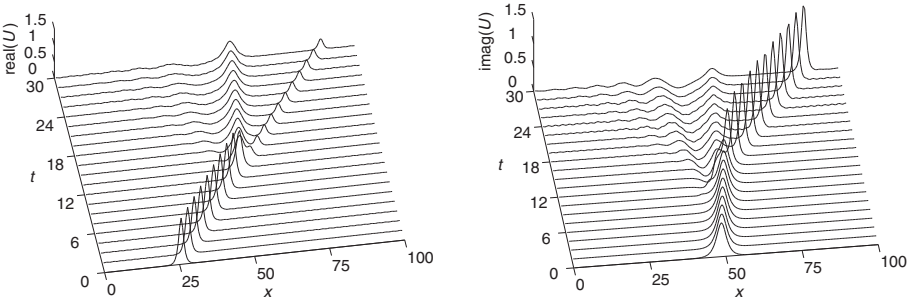

FIGURE 5. Real and imaginary parts of the solution. Left: real part, right: imaginary part.

4.2. Interaction of two solitary waves In this example, we consider the interaction of two solitary waves; the initial condition is given by (see, for example, [16])

$$u(x,0) = \sqrt{\frac{2c_1}{\alpha}}\,\mathrm{sech}(\sqrt{c_1}(x-x_1))\exp(i\theta_1) + \sqrt{\frac{2c_2}{\alpha}}\,\mathrm{sech}(\sqrt{c_2}(x-x_2))\exp(i\theta_2),$$

where α, c_i, θ_i and x_i $(i = 1, 2)$ are given constants. The solution corresponds to two solitary waves, one initially located at x_1, while the other is at x_2 and both are travelling to the right with velocity c_i $(i = 1, 2)$. The problem is solved in the interval $[0, 100]$; we set $\alpha = 2$, $x_1 = 25$, $x_2 = 48$, $c_1 = 2$, $c_2 = 0.5$, and the computation is done up to time $T = 30$.

Firstly, we consider the interaction between a y-polarized solitary wave ($\theta_1 = 0$) and a z-polarized solitary wave ($\theta_2 = \pi/2$). The interaction profile is presented in Figure 4. Notice that the taller wave moves faster than the shorter one; it catches up and collides with the shorter wave and then moves ahead from the shorter wave. We also note that there is a small tail following the shorter wave after the interaction, which agrees with the result obtained by Uddina et al. [19]. Figure 5 presents the real and imaginary parts of the numerical solution. The relative errors of discrete mass and energy are plotted in Figure 6, which are in good agreement with the theoretical results.

https://doi.org/10.1017/S1446181120000218 Published online by Cambridge University Press

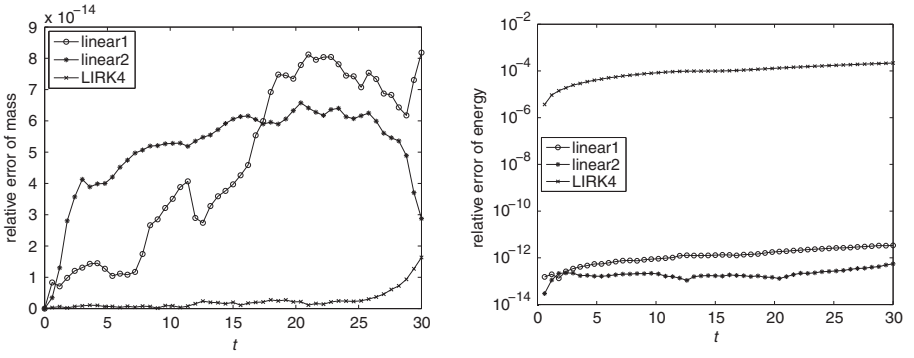

FIGURE 6. Time evolution of the relative errors of discrete mass and energy. Left: $|M(t) - M(0)|/M(0)$; right: $\log(|\widetilde{H}(t) - \widetilde{H}(0)|/\widetilde{H}(0))$.

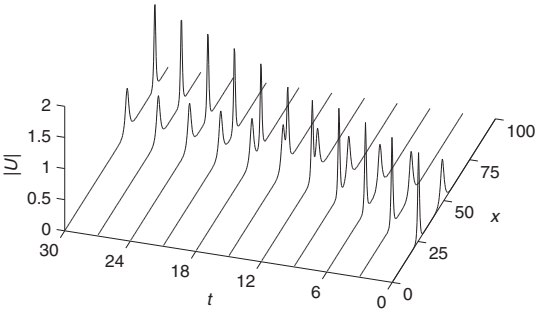

FIGURE 7. Numerical solution of the linear1 when $h = 1/2$, $\tau = 0.01$ and $\theta_1 = \theta_2 = 0$.

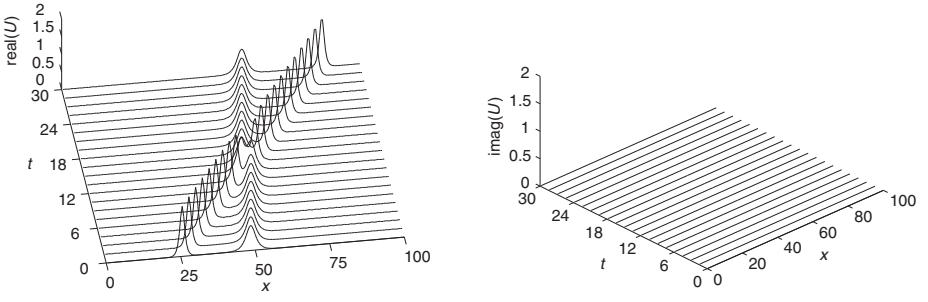

FIGURE 8. Real and imaginary parts of the solution. Left: real part; right: imaginary part.

Secondly, we study the interaction of two y-polarized solitary waves ($\theta_1 = \theta_2 = 0$) (see, for example, [18]). The interaction profile is shown in Figure 7. We find that the solitary waves preserve their amplitudes very well and there is no small trail. Therefore, we conclude that the interaction is elastic, which is in good agreement with those reported by Muslu and Erabay [18] and Uddina et al. [19]. Figure 8 presents the real and imaginary parts of the solution. It is noted that the imaginary part is

https://doi.org/10.1017/S1446181120000218 Published online by Cambridge University Press

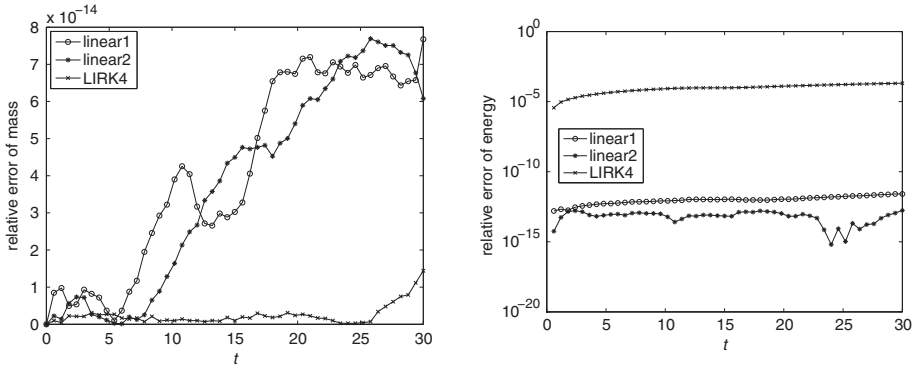

FIGURE 9. Time evolution of the relative errors of discrete mass and energy. Left: $|M(t) - M(0)|/M(0)$; right: $\log(|\widetilde{H}(t) - \widetilde{H}(0)|/\widetilde{H}(0))$.

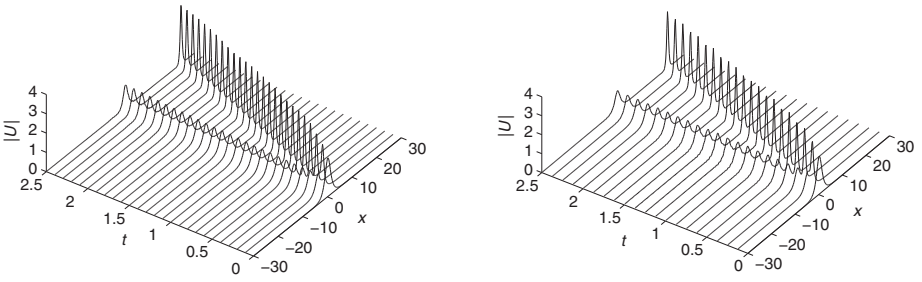

FIGURE 10. Numerical solutions of the linear1 and the LIRK4 methods. Left: the linear1 method with $h = 1/2$, $\tau = 0.01$; right: the LIRK4 method with $h = 1/4$, $\tau = 0.001$.

zero, which agrees with the exact solution. The relative errors of discrete mass and energy are plotted in Figure 9, which shows that the proposed schemes can conserve the discrete mass and energy to machine precision. On the contrary, the LIRK4 method can only conserve energy within 10^{-5}.

4.3. Wave break-up In this example, we consider the wave break-up phenomenon [16]. The initial condition is given as follows:

$$u(x, 0) = \sqrt{\frac{2c}{\alpha}}\,\mathrm{sech}(x)\exp(i\theta_0),$$

where α, θ_0 and c are given constants. The solution represents a solitary wave with amplitude $\sqrt{2c/\alpha}$, initially located at $x = 0$, and is moving to the right with velocity $c = 1$. We set

$$\alpha = 2, \quad \theta_0 = \pi/4, \quad -30 \le x \le 30, \quad T = 2.5, \quad h = 1/2, \quad \tau = 0.01.$$

The numerical solutions of the linear1 and LIRK4 methods are presented in Figure 10. We observe that the solitary wave breaks up into two solitary waves, and

https://doi.org/10.1017/S1446181120000218 Published online by Cambridge University Press

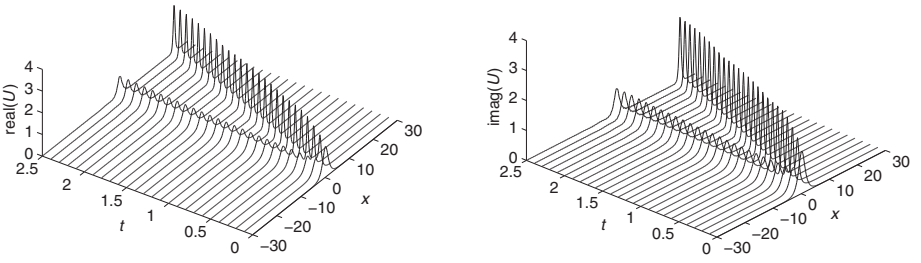

FIGURE 11. Real and imaginary parts of the linear1. Left: real part; right: imaginary part.

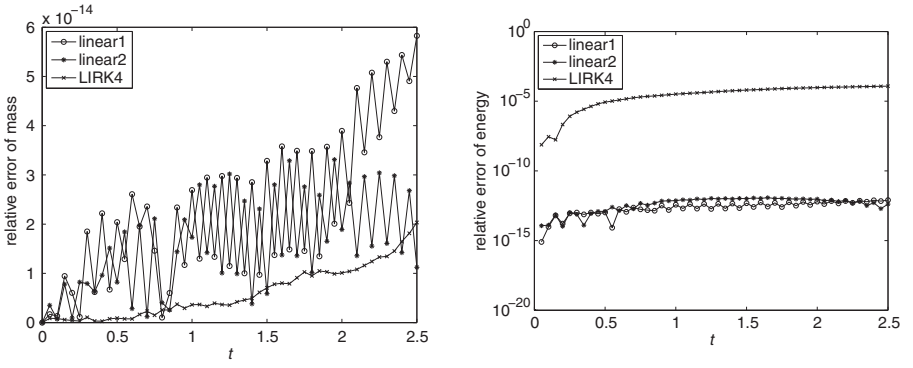

FIGURE 12. Time evolution of the relative errors of discrete mass and energy. Left: $|M(t) - M(0)|/M(0)$; right: $\log(|\widetilde{H}(t) - \widetilde{H}(0)|/\widetilde{H}(0))$.

becomes thinner and higher in comparison with the initial state. Note that the distance between two solitary waves becomes larger and larger as time passes. The results agree well with those reported by Korkmaz and Dağ [16]. The real and imaginary parts of the numerical solution are presented in Figure 11, which shows similar phenomena. The results obtained by the LIRK4 method are similar to those obtained by the proposed schemes, but it needs smaller space and time steps. Therefore, we can conclude that our schemes have better stability than the LIRK4 method. The relative errors of discrete mass and energy are displayed in Figure 12, which are conserved very well.

5. Conclusions

In this paper, two linearly implicit energy-preserving schemes are proposed for the CMKDV equation. The proposed schemes are robust and suitable for long-time computation. The schemes are easy to implement, since these only need to solve a linear system at each time step. Numerical results show that our schemes can reach an arbitrary order of accuracy in space and second-order accuracy in time. More importantly, the proposed schemes can conserve the discrete mass and energy to

https://doi.org/10.1017/S1446181120000218 Published online by Cambridge University Press

machine precision. The comparisons with some existing methods further confirmed that our schemes have better stability and conservation properties.

Acknowledgements

This work is partially supported by the National Natural Science Foundation of China (Grant Nos. 11861047, 41901323 and 11801226), the Natural Science Foundation of Fujian Province (Grant No. 2019J01831), the PhD Start-up Fund of Wuyi University (Grant No. YJ201702) and Jiangsu Key Laboratory for NSLSCS (Grant No. 201804). The authors would like to thank Professor S. R. Clarke for his help during the programme of the linearly implicit Runge–Kutta method. The authors are also grateful to the anonymous reviewers for their insightful comments and suggestions.

References

[1] J. X. Cai and J. Miao, "New explicit multisymplectic scheme for the complex modified Korteweg–de Vries equation", *Chin. Phys. Lett.* **29** (2012) 030201; doi:10.1088/0256-307X/29/3/030201.

[2] W. J. Cai, C. L. Jiang and Y. S. Wang, "Structure-preserving algorithms for the two-dimensional sine-Gordon equation with Neumann boundary conditions", *J. Comput. Phys.* **395** (2019) 166–185; doi:10.1016/j.jcp.2019.05.048.

[3] M. P. Calvo, J. De Frutos and J. Novo, "Linearly implicit Runge–Kutta methods for advection–reaction–diffusion equations", *Appl. Numer. Math.* **37** (2001) 535–549; doi:10.1016/S0168-9274(00)00061-1.

[4] J. B. Chen and M. Z. Qin, "Multi-symplectic Fourier pseudospectral method for the nonlinear Schrödinger equation", *Electron. Trans. Numer. Anal.* **12** (2001) 193–204, available at http://etna.mcs.kent.edu/volumes/2001-2010/vol12/.

[5] S. Erbay and E. S. Suhubi, "Nonlinear wave propagation in micropolar media II. Special cases, solitary waves and Painlevé analysis", *Internat. J. Engrg. Sci.* **27** (1989) 915–919; doi:10.1016/0020-7225(89)90032-3.

[6] D. Furihata and T. Matsuo, *Discrete variational derivative method: a structure-preserving numerical method for partial differential equations*, (CRC Press, London, 2010).

[7] Y. Z. Gong and J. Zhao, "Energy-stable Runge–Kutta schemes for gradient flow models using the energy quadratization approach", *Appl. Math. Lett.* **94** (2019) 224–231; doi:10.1016/j.aml.2019.02.002.

[8] Y. Z. Gong, J. Zhao and Q. Wang, "Arbitrarily high-order unconditionally energy stable SAV schemes for gradient flow models", *Comput. Phys. Comm.* **249** (2020) 107033; doi:10.1016/j.cpc.2019.107033.

[9] Y. Z. Gong, J. Zhao and Q. Wang, "Arbitrarily high-order unconditionally energy stable schemes for thermodynamically consistent gradient flow models", *SIAM J. Sci. Comput.* **42** (2020) B135–B156; doi:10.1137/18M1213579.

[10] Y. Z. Gong, J. Zhao, X. F. Yang and Q. Wang, "Fully discrete second-order linear schemes for hydrodynamic phase field models of binary viscous fluid flows with variable densities", *SIAM J. Sci. Comput.* **40** (2018) B138–B167; doi:10.1137/17M1111759.

[11] O. B. Gorbacheva and L. A. Ostrovsky, "Nonlinear vector waves in a mechanical model of a molecular chain", *Physica D* **8** (1983) 223–228; doi:10.1016/0167-2789(83)90319-6.

[12] Q. Hong, Y. Z. Gong and Z. Q. Lv, "Linear and Hamiltonian-conserving Fourier pseudo-spectral schemes for the Camassa–Holm equation", *Appl. Math. Comput.* **346** (2019) 86–95; doi:10.1016/j.amc.2018.10.043.

[13] M. S. Ismail, "Numerical solution of complex modified Korteweg–de Vries equation by Petrov–Galerkin method", *Appl. Math. Comput.* **202** (2008) 520–531; doi:10.1016/j.amc.2008.02.033.

[14] M. S. Ismail, "Numerical solution of complex modified Korteweg–de Vries equation by collocation method", *Commun. Nonlinear Sci. Numer. Simul.* **14** (2009) 749–759; doi:10.1016/j.cnsns.2007.12.005.

[15] C. F. F. Karney, A. Sen and F. Y. F. Chu, "Nonlinear evolution of lower hybrid waves", *Phys. Fluids* **22** (1979) 940–952; doi:10.1063/1.862688.

[16] A. Korkmaz and İ. Dağ, "Solitary wave simulations of complex modified Korteweg–de Vries equation using differential quadrature method", *Comput. Phys. Comm.* **180** (2009) 1516–1523; doi:10.1016/j.cpc.2009.04.012.

[17] I. A. Korostil and S. R. Clarke, "Fourth-order numerical methods for the coupled Korteweg–de Vries equations", *ANZIAM J.* **56** (2014), 275–285; doi:10.1017/S1446181115000012.

[18] G. M. Muslu and H. A. Erabay, "A split-step Fourier method for the complex modified Korteweg–de Vries equation", *Comput. Math. Appl.* **45**(2003) 503–514; doi:10.1016/S0898-1221(03)80033-0.

[19] M. Uddina, S. Haqa and S. U. Islam, "Numerical solution of complex modified Korteweg–de Vries equation by mesh-free collocation method", *Comput. Math. Appl.* **58** (2009) 566–578; doi:10.1016/j.camwa.2009.03.104.

[20] J. L. Yan and L. H. Zheng, "Conservative finite volume element schemes for the complex modified Korteweg–de Vries equation", *Int. J. Appl. Math. Comput. Sci.* **27** (2017) 515–525; doi:10.1515/amcs-2017-0036.

[21] X. F. Yang, J. Zhao and Q. Wang, "Numerical approximations for the molecular beam epitaxial growth model based on the invariant energy quadratization method", *J. Comput. Phys.* **333** (2017) 104–127; doi:10.1016/j.jcp.2016.12.025.

[22] H. Zhang, X. Qian, J. Y. Yan and S. H. Song, "Highly efficient invariant-conserving explicit Runge–Kutta schemes for nonlinear Hamiltonian differential equations", *J. Comput. Phys.* **418** (2020) 109598; doi:10.1016/j.jcp.2020.109598.

[23] J. Zhao, X. Yang, Y. Gong, X. Zhao, X. Yang, J. Li and Q. Wang, "A general strategy for numerical approximations of non-equilibrium models—part I: thermodynamical systems", *Int. J. Numer. Anal. Model.* **15** (2018) 884–918, available at https://doc.global-sci.org/uploads/Issue/IJNAM/v6n15/615_884.pdf.